Article

Bull. Volcanol. Soc. Japan
Vol. 58 (2013) No. 1, pp. 43−58

Geochemical and Sr-Nd-Pb Isotopic Constraints on the Origin and Magmatic Evolution of Quaternary Lavas of Sakurajima Volcano, Southern Kyushu Island, Japan

Tomoyuki SHIBATA*, Jun SUZUKI*, Masako YOSHIKAWA*, Tetsuo KOBAYASHI**, Daisuke MIKI*** and Keiji TAKEMURA*

(Received October 5, 2011; Accepted January 7, 2013)

We present the results of a detailed petrogenetic study employing newly determined whole-rock major and trace element geochemical analyses and Sr-Nd-Pb isotopic compositions of andesitic and dacitic Quaternary lavas of Sakurajima volcano, a post-caldera volcano situated within the Aira caldera of Japan. Similar geochemical and isotopic investigations are also carried out on basaltic rocks from pre-caldera stage and monogenetic volcanoes from near Sakurajima volcano. Quaternary lavas of Sakurajima volcano analyzed in this study are classified as porphyritic andesites or dacites that contain a mineral assemblage of orthopyroxene, clinopyroxene, and plagioclase, with or without olivine, in a groundmass exhibiting either hyalo-ophitic or hyalopilitic textures. The trace element characteristics of these samples are similar to those of typical island arc magmas, showing clear evidence of Nb depletion along with enrichments in Rb, K, and Pb, which suggests the addition of aqueous fluids to the mantle wedge during melt generation. The Sr, Nd, and Pb isotopic compositions plot close to a mixing curve between MORB-type mantle and sediments of the Philippine Sea Plate, but displaced a bit towards more radiogenic compositions. Plots of Zr versus Nb concentration in these lavas yield a linear trend that falls on a compositional mixing line between the values for mid-ocean ridge basalt (MORB) and average continental crust. Collectively, these observations indicate that the primary source magmas for the Quaternary lavas of Sakurajima volcano were initially generated by partial melting of MORB-type mantle wedge that had already been hydrated by fluids derived from the subducting Philippine Sea Plate. The additional contribution of significant amounts of crustal material during magma evolution is also evident from the Zr/Nb ratios and Sr-Nd-Pb isotopic compositions of the analyzed andesites and dacites of Sakurajima lava samples. From the mixing relation of Sr-Nd-Pb isotopic compositions, it is suggested that the sedimentary rocks of Shimanto Group can be a source of the crustal materials. Although most of the major element oxide compositions of these lavas show a single linear trend on each of the Harker diagrams, two different trends are clearly discernible on each of the P_2O_5, and TiO_2 versus silica variation diagrams, and are subdivided into low-P and high-P geochemical groups. These two groups can also be distinguished when comparing their P_2O_5 and TiO_2 contents and $^{87}Sr/^{86}Sr$ ratios, relative to their phenocrystic plagioclase modal abundances. The magma mixing trends of Sakurajima lavas, which seem to be extended from mono andesitic end-member to two different deictic end-members, are observed from the relationships of major element contents and $^{87}Sr/^{86}Sr$ ratios. In addition, the low-P versus high-P groups of lavas show distinctive distribution patterns, whereby the high-P lavas are surrounded by low-P lavas in the central to southern parts of the Sakurajima volcano study area. These observations indicate that mixing of andesitic and dacitic magmas played an important role in the genesis of Quaternary lavas of Sakurajima volcano, and that multiple dacitic magma chambers with different geochemical characteristics once existed beneath the Sakurajima area at relatively shallow levels in the crust. From the relations between SiO_2 and Sr isotope ratios, an assimilation and fractional crystallization process is required to originate the andesite and dacite end-members.

Key words: Sakurajima volcano; Aira; Kyushu; caldera; arc magmas; trace elements; Sr-Nd-Pb isotopes

* Beppu Geothermal Research Laboratory, Institute for Geothermal Sciences, Kyoto University, Beppu, Oita 874−0903, Japan.
** Graduate School of Science and Engineering, Kagoshima University, Kagoshima, Kagoshima 890−0065, Japan.
*** Sakurajima Volcano Research Center, Disaster Prevention Research Institute, Kyoto University, Sakurajima, Kagoshima 891−1419, Japan.

Corresponding author: Tomoyuki Shibata
e-mail: tomo@bep.vgs.kyoto-u.ac.jp

1. Introduction

Volcanic eruptions and associated caldera formation represent some of the most catastrophic geological phenomena on Earth, and hence many geological, petrological, geochemical, and geophysical studies have sought to understand these phenomena (*e.g.*, Smith and Bailey, 1968; Lipman, 1984; Furukawa *et al*., 2009; Gregg *et al*., 2012). From these studies, it is now well established that huge volumes of silicic magmas accumulate beneath the volcano prior to caldera formation, and that eruptions of pyroclastic material are typically caused by some sort of obvious trigger (*e.g.*, Hildreth and Wilson, 2007). However, the origin of the silicic magmas themselves is more controversial, and several petrogenetic models have been proposed, as follows; 1) fractional crystallization of mafic magma with crustal assimilation (AFC model; *e.g.*, DePaolo, 1981; Caffe *et al*., 2002; Reagan *et al*., 2003), 2) partial melting of basaltic lower crust (*e.g.*, Takahashi, 1986; Bead and Lofgren, 1991) and 3) partial melting of basaltic rocks that were emplaced into the lower crust a long time prior to the actual silicic magma activity itself (*e.g.*, Sisson *et al*., 2005; Ban *et al*., 2007). Investigations into the nature and origin of different magmas that may have been generated pre-, syn-, or post-caldera formation, are particularly useful for understanding the genesis of these types of silicic magmas, especially because there is the distinct possibility that such silicic magmatic and volcanic activity could be the harbinger of the next caldera-forming event (*e.g.*, Furukawa *et al*., 2009; Miyoshi *et al*., 2011).

Sakurajima volcano represents a post-caldera volcano linked with the Aira caldera, which itself is situated along the volcanic front of the Ryukyu arc, at the southern end of Kyushu Island, Japan (Fukuyama, 1978), where the Philippine Sea Plate (PSP) is subducting beneath the Eurasian Plate (Fig. 1). After the formation of the Aira caldera at ca. 29 cal ka BP, volcanism associated with Sakurajima volcano at about 26 cal ka BP, which to this day remains an active volcano (Okuno, 2002). For this reason, Sakurajima volcano is considered to be one of the most suitable volcanoes for studying the links between caldera formation and catastrophic silicic magmatic activity. It has been proposed that the relative contributions of basaltic, andesitic, and dacitic magmas are reflections of the assimilation of variable amounts of crustal materials, and this relationship is thought to explain the entire process of magmatic evolution of the Sakurajima lavas subsequent to their initial formation by slab-fluid-related partial melting in the mantle wedge (Yanagi *et al*., 1991; Arakawa *et al*., 1998; Uto *et al*., 2005; Nakagawa *et al*., 2011). Yanagi *et al*. (1991) emphasized that a binary magma-mixing process must have played an important role in producing the observed linear trends of the Sakurajima lavas on plots of major element oxides versus SiO_2 content (Fig. 2), as well as the commonly observed bimodal anorthite contents within the phenocrystic plagioclase cores of these lavas. Arakawa *et al*. (1998) reported an observed increase in $^{87}Sr/^{86}Sr$ ratio with increasing SiO_2 content for the volcanics of the Aira caldera (including Sakurajima lavas), and suggested that the contribution of crustal materials to the magma at some stage of its evolution can explain these geochemical/isotopic relationships. They also emphasized that magma mixing of mantle-derived basaltic magma with dacitic magma that had interacted with lower crustal materials, may have taken place during the magmatic evolution of these magmas. Recently, Uto *et al*. (2005) noted that two distinct geochemical trends are discernible on several plots of major oxide compositions versus SiO_2 content, especially with regards to TiO_2 and P_2O_5 concentrations. They also identified two distinct trends on diagrams displaying SiO_2 content versus $^{87}Sr/^{86}Sr$ ratio; i.e., both low and high $^{87}Sr/^{86}Sr$ ratios for different rocks with the same SiO_2 concentrations, and therefore claimed that more complicated magmatic evolutionary processes are required to explain the data. Therefore, geochemical evolution of Sakurajima lavas is still controversial. However, the available geochemical data on lavas erupted from Sakurajima volcano are currently somewhat limited in terms of elucidating robust petrogenetic models of silicic magma generation linked with this volcano-caldera system. Although considerable amounts of major and trace element geochemical data have been reported for this volcano, and several Sr-Nd isotopic datasets are also available (*e.g.*, Arakawa, 1998; Uto *et al*., 2005), data on Pb isotopic ratios of these lavas, which would be useful in deciphering the magma source materials (*e.g.*, Shibata and Nakamura, 1997) are currently rather scarce.

In the present study, we collected several volcanic rock samples (mainly lavas), from almost all of the individual volcanostratigraphic units (Table 1; Fig. 1) previously defined by Fukuyama and Ono (1981), for a detailed whole-rock major and trace element geochemical and Sr-Nd-Pb isotopic petrogenetic investigation of Quaternary lavas of Sakurajima volcano. In addition to these Sakurajima samples, we studied basaltic volcanic rocks collected from a region adjacent to the Aira caldera, in order to obtain information of the primary magmas linked with the formation of Sakurajima volcano.

2. Sample descriptions

Sakurajima volcano consists of two adjoined stratovolcanoes; Kitadake and Minamidake. Kitadke volcano is further subdivided into two separate volcanic edifices known as “Old” Kitadake volcano and “Young” Kitadake volcano, which were active from ～26 to 24 cal ka BP and from 12.8 to 5 cal ka BP, respectively (Okuno, 2002). Minamidake volcano is an active stratocone that has been growing on the southern slope of Kitadake since about 4.5 cal ka BP (Okuno, 2002). In addition, a number of smaller parasitic volcanoes are observed that have been described

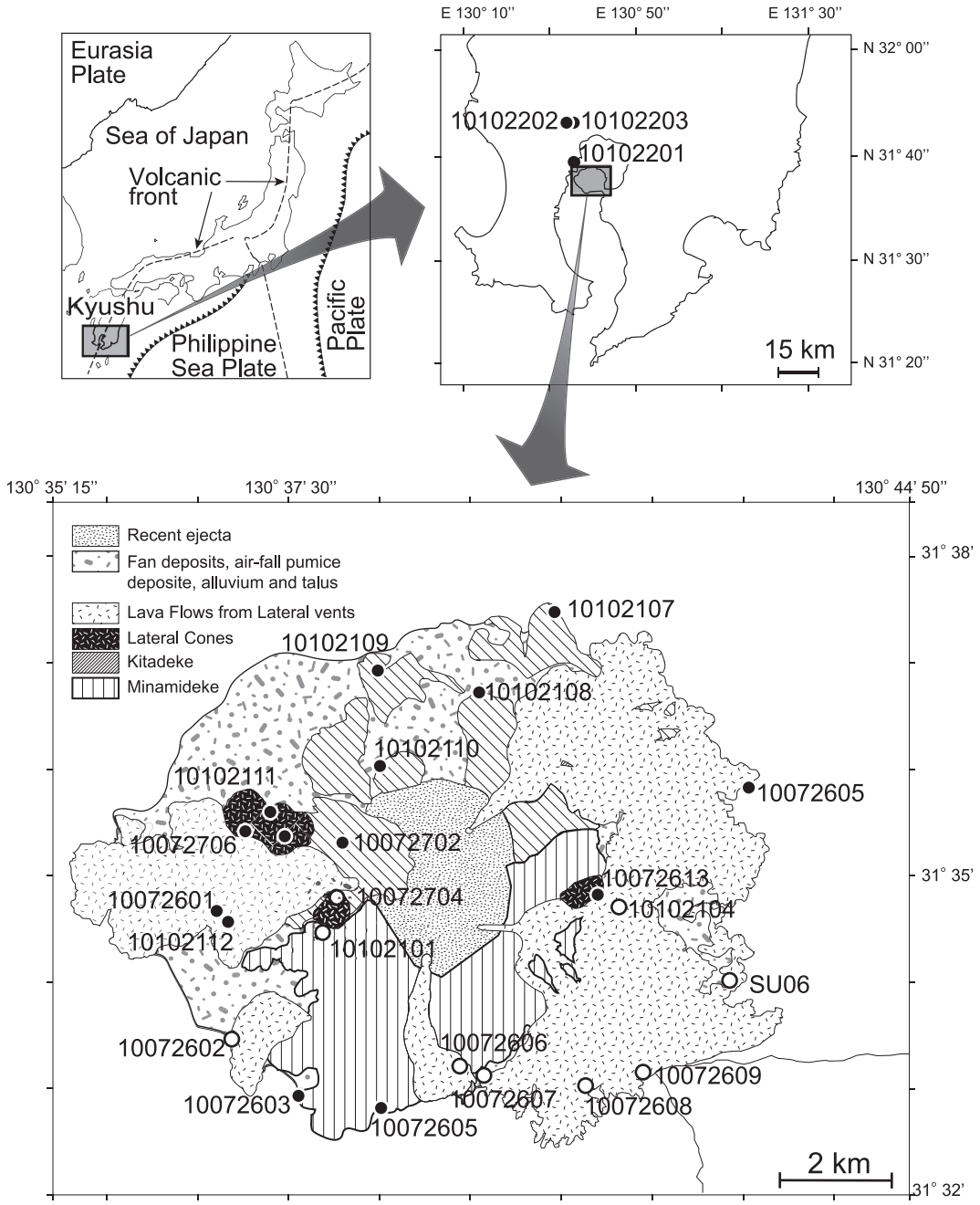

Fig. 1. Geological context and sampling localities. The volcanostratigraphic succession of Sakurajima volcano is simplified from Fukuyama and Ono (1981). Solid and open circles represent low-P and high-P groups, respectively (see main text for details).

as the lateral cones and lava flows from lateral vents, respectively, by (Fukuyama, 1978), with the latter having erupted in historical times (except for the Atagoyama lavas). From all of these various volcanic structures and flows, the volcanics of Sakurajima volcano are classified into four distinct groups; Kitadake, Minamidake, lateral cones, and lateral vents. Fukuyama and Ono (1981) subdivided these four groups into 27 units on the basis of

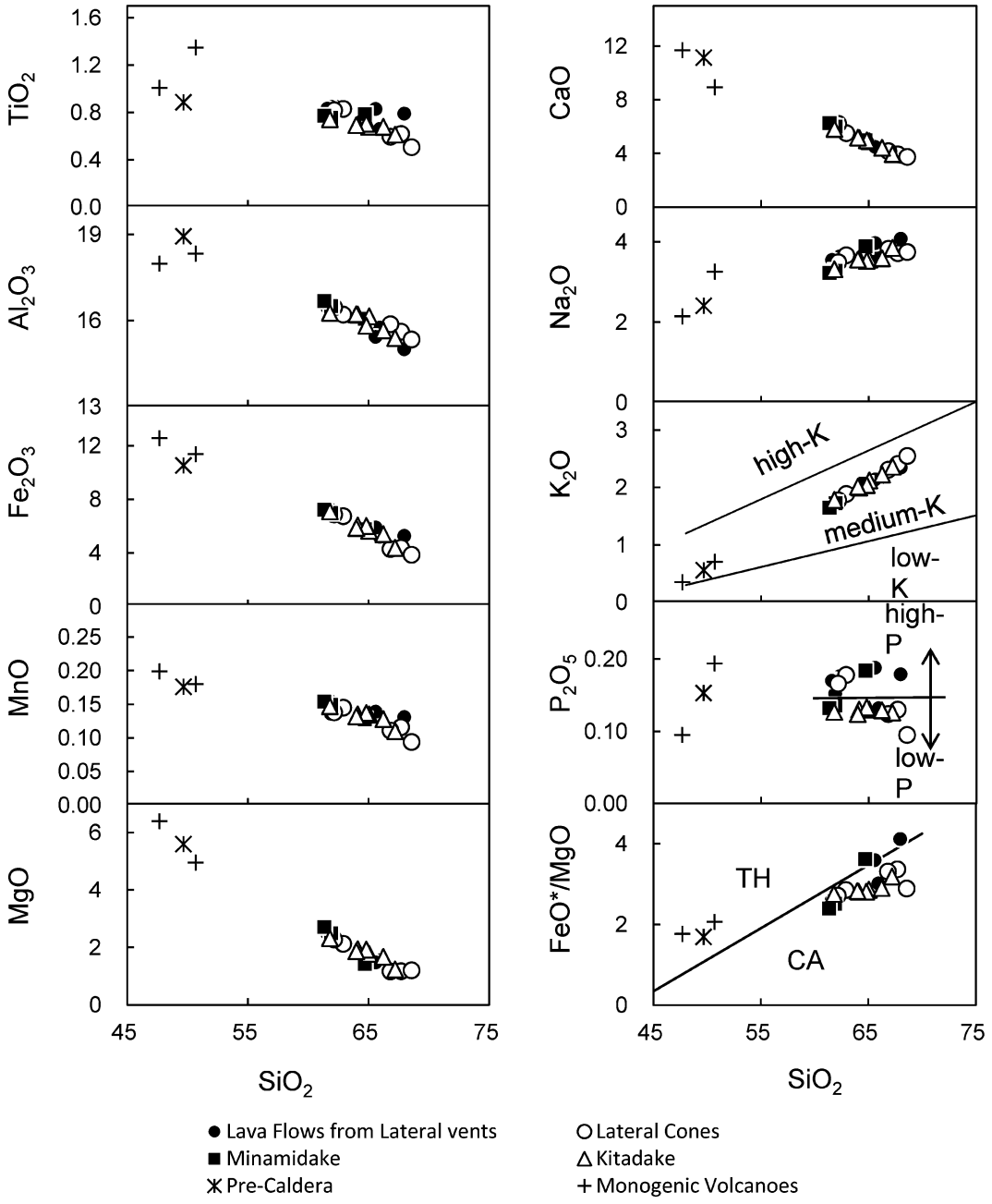

Fig. 2. Plots of SiO_2 versus major element oxides (and FeO*/MgO ratio). All oxides are presented in wt.%. TH and CA denote tholeiite and calc-alkaline rock series, respectively. See the main text for additional information on TH, CA, low-K, medium-K, and high-K series.

lithologic, geographic and stratigraphic relationships. Fukuyama and Ono (1981) also described that 22 of the 27 volcanostratigraphic units of Sakurajima volcano are composed of lava flows and/or lava domes, whereas the other 5 units (including the Harutayama unit) are composed of pyroclastics. Subsequent to that study, Kobayashi (1982) revealed that the Harutayama unit is actually made up of a lava dome rather than pyroclastics. Thus, there are now 23 units that are considered to be composed of lava flows and/or lava domes; all of these were sampled in the

Table 1. Stratigraphic succession and sample localities.

		Lava unit	Rock Type	Age	Locality	*Group
Post Caldera Stage	Lava Flows from Lateral Vents	Showa Lava	Opx-Cpx Andeite	1946 A.D.	31° 33' 19.3" N 130° 40' 00.6" E	high-P
		Taisho Lava - II	Opx-Cpx Andeite	1914 A.D.	31° 33' 13.4" N 130° 41' 07.8" E	high-P
		Taisho Lava - I	Opx-Cpx Andeite		31° 33' 20.3" N 130° 41' 45.1" E	high-P
		An-ei Lava	Opx-Cpx Dacite	1779 A.D.	31° 33' 24.7" N 130° 39' 44.6" E	high-P
		Bunmei Lava - II	Opx-Cpx Dacite	1475-1476 A.D.	31° 36' 01.8" N 130° 42' 54.8" E	high-P
		Bunmei Lava - I		1471 A.D.		
		Atagoyama Lava	Opx-Cpx Dacite		31° 34' 46.3" N 130° 37' 11.5" E	low-P
		Nagasakibana Lava	Cpx-Opx Andeite	746 - 766 A.D.	31° 34' 12.9" N 130° 42' 42.3" E	
	Lateral Cones	Nabeyama Pumice Cone	Opx-Cpx Andeite		31° 34' 54.4" N 130° 41' 29.5" E	high-P
		Gongenyama Lava Dome	Opx-Cpx Dacite		31° 35' 01.3" N 130° 41' 15.6" E	low-P
		Hikinohira Lava Dome	Cpx-Opx Andeite		31° 34' 59.9" N 130° 38' 23.7" E	high-P
		Harutayama Lava Dome	Opx-Cpx Dacite			
		Yunohira Lava Dome	Cpx-Opx Dacite		31° 34' 59.9" N 130° 37' 49.7" E	low-P
		Furihatayama Lava Dome	Cpx-Opx Dacite		31° 34' 59.9" N 130° 37' 23.5" E	low-P
	Minamidake Volcano	M4 Lava (Ohhira Lava)	Opx-Cpx Dacite		31° 34' 39.5" N 130° 38' 13.8" E	high-P
		Minamidake Lava and Pyroclastics				
		Kannonzaki Lava	Opx-Cpx Andeite	3 ka	31° 33' 00.2" N 130° 38' 52.7" E	low-P
		Miyamoto Lava	Opx-Cpx Andeite	4ka	31° 33' 07.9" N 130° 37' 58.8" E	low-P
	Kitadake Volcano	K8 Lava	Opx-Cpx Dacite		31° 36' 13.7" N 130° 38' 52.0" E	low-P
		K7 Lava and Pyroclastics				low-P
		K6 Lava	Opx-Cpx Andeite		31° 36' 55.7" N 130° 39' 57.6" E	low-P
		Uwatoko Lava	Opx-Cpx Dacite		31° 35' 30.1" N 130° 38' 27.1" E	low-P
		Fujino Lava	Opx-Cpx Dacite			low-P
		Wariishizaki Lava	Opx-Cpx Dacite		31° 37' 41.0" N 130° 40' 47.5" E	low-P
		Matsuura Lava	Cpx-Opx Dacite		31° 37' 08.0" N 130° 38' 50.4" E	low-P
		Kitadake Pyroclastics				low-P
Pre-caldera		Shirahama Basalt	Cpx Basalt	0.93±0.35 Ma	31° 38' 46.2" N 130° 36' 00.5" E	
Monogenetic volcano		Aojiki Basalt	Cpx Basalt	0.08±0.02 Ma	31° 46' 22.5" N 130° 34' 19.6" E	
		Sumiyoshiike Basalt	Cpx Basalt	7,200 yrs BP	31° 46' 11.7" N 130° 35' 20.2" E	

*: Sample are dividred into low- and hjig-P on tne basis of P_2O_5 content. See texet in the detailes.
Gray characters show uncollected samples. Ages are from Uto et al. (2005), Inoue et al. (1994), Shuto et al. (2001) and Kobayashi and Tameike (2002).

present geochemical and isotopic study of Sakurajima volcano. Because the rock types represented by all of these lava samples fall in a restricted range of compositions from andesitic to dacitic, we also sampled basaltic rocks from pre-caldera stage lavas of the Aira caldera and from associated monogenetic volcanoes adjacent to Sakurajima volcano, in order to investigate the chemical characteristics of the mantle wedge beneath the study area. All of these sample localities are shown in Fig. 1. Petrographic observations of these historical lava samples, as made in the present study, compare favorably with those presented by Kubotera (1981). Because no remarkable petrographic differences are observed amongst the various volcanic stages/units of Sakurajima volcano, the descriptions of the lava samples analyzed in this study are simply made as a broad description for each rock type, although the modal abundances (of both the mineralogical constituents and groundmass) for each individual sample are listed in Table 2.

2−1 Dacites

The analyzed dacite samples comprise gray- to black-colored porphyritic volcanic rocks that exhibit hyalo-ophitic or hyalopilitic groundmasses with exceptions of the Matsura and K8 lavas, which show hyalopilitic groundmasses that often contain vesicles. Several dacite samples of the Matsura and Atagoyama lavas show a distinct fluidal structure, while a number of others exhibit only a weak fluidal structure. The phenocrysts within these dacites exhibit a wide range of grain sizes from <0.1 to 2.0 mm across, which to some degree correlates with crystal habit, whereby the relatively large phenocrysts tend to be euhedral and the smaller ones subhedral to anhedral. The phenocrysts consist of orthopyroxene (Opx), clinopyroxene (Cpx), plagioclase (Pl), and opaque minerals (Opq). According to Fukuyama (1981), the Opq that occur within the historic lavas commonly contain titanomagnetite crystals. The groundmass consists primarily of brown to dark brown volcanic glass, with lesser amounts of microcrystalline Pl, Opx, Cpx, and Opq. Brown to dark brown glass inclusions often occur within the Pl phenocrysts.

2−2 Andesites

The andesite samples analyzed in this study are mainly gray to black in color, exhibiting porphyritic textures with hyalo-ophitic groundmasses, and are often vesiculated. Similarly to those in the dacite samples, the phenocrysts in these rocks show a wide range of grain sizes from <0.1 to 2.0 mm across, with relatively large phenocrysts being euhedral and smaller phenocrysts being subhedral to anhedral. The andesites contain discrete phenocrystic grains of Opx, Cpx, Pl, and Opq, although the rock samples collected from the Taisho I and Atogoyama lava flows additionally contain small amounts of olivine (Ol) phenocrysts (Table 2). Kubotera (1981) reported Ol microphenocrysts in the Bunmei andesite lavas, although in the present study we observed no such Ol microphenocrysts in our Bunmei II thin section. The groundmass in these Sakurajima andesites consists predominantly of dark brown glass, along with lesser amounts of Pl, Opx, Cpx, and Opq. Brown to dark brown inclusions of glass are common within Pl phenocrysts.

2−3 Basalts

The Shirahama basalt unit was one of the most dominant types among the lavas which built up the pre-Aira-caldera volcano. The Aojiki and Sumiyoshiike basalts form a part of a suite of monogenetic volcanoes located ~20 km north-northwest of Sakurajima volcano. Phenocrysts in the Shirahama and Sumiyoshiike basalts are relatively coarse-grained at around 2 mm across, whereas those in the Aojiki basalt are comparatively fine-grained at <1 mm across. The basalts sampled in this study commonly show a porphyritic texture with phenocrysts of Ol, Opx, Cpx, Pl, and Opq. The groundmass within the Aojiki basalt shows a discernible intergranular texture consisting of Pl, Cpx, and Opq crystals, whereas the other basalt samples exhibits an intersertal texture made up of Pl, Cpx, Opq, and glass. The plagioclase phenocrysts in the Aojiki basalt exhibit a distinct poikilitic texture defined by numerous small inclusions of glass and anhedral Cpx grains.

3. Whole-rock analytical methods

Prior to whole-rock geochemical and Sr-Nd-Pb isotopic analyses, all rock samples were crushed to coarse chips ($\approx 0.5\,mm^3$), and then fresh pieces were handpicked for each whole-rock aliquot. To avoid surface contamination, the rock chips selected for analysis were then leached with ethanol, 0.5 M HCl, and submerged and rinsed with Milli Q® water in an ultrasonic bath. The clean rock chips were then comminuted to a grain-size of less than 200 mesh using a vibrating tungsten carbide puck mill for the major element chemical analysis, whereas a puck mill made of alumina ceramics was employed to the samples for the trace element and Sr-Nd-Pb isotopic analysis.

Major and trace element whole-rock compositions were determined using a RIGAKU 3070® X-Ray Fluorescence (XRF) system by employing the glass beads and pressed pellets methods, respectively, following closely the procedures and instrumental set-up outlined in Sugimoto *et al*. (2007). Whole-rock Pb, Nd, and Sr isotopic compositions were measured using a Finnigan MAT 262® Thermal Ionization Mass Spectrometer (TIMS) after the methods outlined in Shibata and Yoshikawa (2004), Shibata and Yoshikawa (2002), and Shibata *et al*. (2007). All of the whole-rock geochemical and isotopic analyses in this study were carried out at the Institute for Geothermal Sciences (IGS), Kyoto University, Japan. The normalizing factors used to correct isotope fractionation during mass spectrometry, in the course of Sr, Nd, and Pb isotopic measurements, were: $^{86}Sr/^{88}Sr = 0.1194$, $^{146}Nd/^{144}Nd = 0.7219$, and 0.001 % per atomic mass unit, respectively. The measured isotopic ratios of the employed standard

Table 2. Whole-rock major oxide and trace element concentrations, and modal mineralogy of Sakurajima volcano lavas and nearby basalts.

	Lava Flows from Lateral vents							Lateral Cones					
Sample No.	10102112	SU06	10072602	10072606	10072609	10072608	10072607	10072706	10102111	HARG54.	10072704	10072613	10102104
Lava Unit	Atagoyama	Nagasaki-bana	Bunmei	Anei	Taisho I	Taisho II	Showa	Furihata-yama	Yunohira	Haruta-yama	Hikinohira	Gongen-yama	Nabeyama
SiO_2(wt.%)	65.93	61.88	67.96	65.58	62.27	61.88	61.58	67.69	66.81	67.20	62.90	68.56	62.15
TiO_2	0.66	0.82	0.79	0.83	0.85	0.85	0.83	0.62	0.60	0.61	0.83	0.51	0.82
Al_2O_3	15.75	16.27	15.00	15.44	16.30	16.26	16.45	15.62	15.87	15.40	16.21	15.34	16.46
Fe_2O_3	5.21	6.98	5.27	5.90	7.02	7.22	7.18	4.39	4.29	4.38	6.75	3.87	6.87
MnO	0.13	0.14	0.13	0.14	0.15	0.15	0.15	0.12	0.11	0.11	0.15	0.09	0.14
MgO	1.56	2.34	1.15	1.48	2.32	2.52	2.49	1.17	1.17	1.24	2.13	1.20	2.28
CaO	4.32	5.98	3.75	4.49	5.85	6.01	6.12	3.93	4.16	3.94	5.51	3.74	6.21
Na_2O	3.64	3.51	4.08	3.97	3.63	3.51	3.55	3.72	3.83	3.85	3.67	3.75	3.49
K_2O	2.15	1.78	2.35	2.14	1.77	1.74	1.71	2.41	2.31	2.36	1.89	2.55	1.78
P_2O_5	0.13	0.15	0.18	0.19	0.18	0.17	0.17	0.13	0.12	0.13	0.18	0.10	0.17
Total	99.48	99.83	100.66	100.15	100.34	100.30	100.22	99.78	99.28	99.22	100.20	99.70	100.36
Cr(ppm)	17	24	14	17	23	19	22	15	13	16	24	18	28
Nb	3	2	3	3	3	3	3	3	3	3	3	3	2
Ni	44	49	43	43	43	44	44	43	43	42	44	43	47
Pb	6	5	6	5	4	4	4	5	6	5	5	6	4
Rb	52	41	56	50	41	40	39	58	57	59	43	60	41
Sr	173	186	163	178	193	192	196	169	176	170	189	155	189
Y	11	11	14	13	11	11	11	9	9	8	11	7	11
Zr	75	70	83	78	66	68	66	77	78	75	68	79	69
Ol (vol. %)	-	-	-	-	tr.	tr.	-	-	-	-	-	-	-
Opx	1	3	1	3	2	3	3	2	3	2	2	1	
Cpx	3	2	1	3	3	3	4	1	2	3	1	1	3
Pl	23	25	12	15	18	23	20	17	19	17	20	14	20
Opq	1	1	1	1	2	1	2	1	1	1	1	tr.	tr.
Gm	73	68	84	78	75	71	71	78	76	77	76	84	76

	Minamidake			Kitadake						Pre-Caldera	Monogenetic Volcanoes	
Sample No.	10072603	10072605	10102101	10102109	10102107	10072707	10072702	10102108	10102110	10102201	10102202	10102203
Lava Unit	Miyamoto	Kannon-zaki	M4	Matsu-ura	Wariishi	Fujino	Uwatoko	K6	K8	Shirahama	Aojiki	Sumiyoshiike
SiO_2(wt.%)	61.89	61.33	64.70	64.11	65.04	64.81	66.23	61.79	63.98	49.66	50.68	47.68
TiO_2	0.76	0.77	0.79	0.70	0.68	0.71	0.68	0.74	0.69	0.89	1.35	1.01
Al_2O_3	16.51	16.68	16.06	16.21	16.15	15.82	15.66	16.27	16.22	18.93	18.33	17.98
Fe_2O_3	6.97	7.23	5.76	6.05	5.65	6.01	5.40	7.10	5.86	10.53	11.37	12.56
MnO	0.15	0.15	0.13	0.14	0.14	0.14	0.13	0.15	0.13	0.18	0.18	0.20
MgO	2.50	2.72	1.43	1.94	1.78	1.93	1.67	2.32	1.86	5.60	4.95	6.40
CaO	6.01	6.28	4.98	5.16	4.91	4.97	4.42	5.82	5.18	11.15	8.93	11.71
Na_2O	3.28	3.23	3.89	3.58	3.56	3.53	3.59	3.32	3.56	2.41	3.26	2.15
K_2O	1.73	1.65	2.07	2.00	2.12	2.04	2.22	1.78	2.01	0.56	0.71	0.35
P_2O_5	0.14	0.13	0.18	0.13	0.13	0.13	0.13	0.13	0.12	0.15	0.19	0.10
Total	99.94	100.18	99.98	100.01	100.15	100.09	100.12	99.41	99.63	100.05	99.96	100.13
Cr(ppm)	35	36	14	24	26	25	18	23	22	49	23	42
Nb	2	2	3	3	3	3	3	2	3	1	5	1
Ni	44	47	44	43	44	48	45	42	43	62	47	64
Pb	5	4	5	5	5	5	5	4	5	2	2	1
Rb	41	40	49	48	52	49	55	42	49	9	7	6
Sr	186	190	186	179	184	173	166	185	181	341	268	237
Y	9	9	12	10	10	10	9	9	10	10	13	9
Zr	61	65	78	67	69	68	75	62	68	53	61	31
Ol (vol. %)	-	tr.	-	-	-	-	-	-	-	2	4	8
Opx	2	4	1	3	3	2	2	2	1	-	-	-
Cpx	4	3	2	2	4	3	2	3	4	6	2	5
Pl	30	27	17	20	22	22	22	25	20	41	27	26
Opq	3	2	1	1	2	2	1	2	1	2	2	tr.
Gm	61	64	80	74	69	71	73	68	74	49	65	60

Total amount of Fe oxide expressed as Fe_2O_3*. The abbreviations Ol, Opx, Cpx, Pl, Opq, and Gm denote olivine, orthopyroxene, clinopyroxene, plagioclase, opaque minerals, and groundmass, respectively. “tr.” and dash “-” denote ‘trace’ and ‘not observed’, respectively.

materials were: $^{87}Sr/^{86}Sr = 0.710279 \pm 0.000028$ (2σ) for NIST SRM987; $^{143}Nd/^{144}Nd = 0.511851 \pm 0.000013$ (2σ) for La Jolla; and $^{206}Pb/^{204}Pb = 16.944 \pm 0.004$ (2σ), $^{207}Pb/^{204}Pb = 15.499 \pm 0.004$ (2σ), and $^{208}Pb/^{204}Pb = 36.721 \pm 0.010$ (2σ) for NIST SRM981.

4. Results

The whole-rock major element compositions of the studied andesitic to dacitic rock samples from Sakurajima volcano (and nearby basalts) are listed in Table 2 and also plotted on silica variation diagrams in Fig. 2. The obtained range of the SiO_2 and MgO contents, and FeO*/MgO

Table 3. Sr, Nd, and Pb isotopic compositions of Sakurajima volcano lavas and nearby basalts.

Volcanic Stage / Lava unit	Sample No.	$^{87}Sr/^{86}Sr$	$^{143}Nd/^{144}Nd$	$^{206}Pb/^{204}Pb$	$^{207}Pb/^{204}Pb$	$^{208}Pb/^{204}Pb$
Kitadake						
Matsuura	10102109	0.705556 ± 0.000013	0.512503 ± 0.000011	18.402 ± 0.002	15.580 ± 0.002	38.646 ± 0.004
Minamidake						
M4	10102101	0.705248 ± 0.000010	0.512554 ± 0.000008	18.381 ± 0.002	15.569 ± 0.001	38.596 ± 0.003
Lava Flows from Lateral vents						
Atago	10102112	0.705690 ± 0.000013	0.512489 ± 0.000009	18.395 ± 0.001	15.571 ± 0.001	38.620 ± 0.003
Nagasakibana	SU06	0.705136 ± 0.000013	0.512543 ± 0.000013	18.385 ± 0.001	15.573 ± 0.001	38.607 ± 0.002
An-ei	10072606	0.705285 ± 0.000014	0.512534 ± 0.000014	18.398 ± 0.001	15.588 ± 0.001	38.658 ± 0.003
Taisho	10072609	0.705208 ± 0.000011	0.512536 ± 0.000015	18.399 ± 0.002	15.591 ± 0.002	38.667 ± 0.004
Showa	10072607	0.705200 ± 0.000011	0.512561 ± 0.000012	18.355 ± 0.001	15.534 ± 0.001	38.485 ± 0.002
Post-calder volcano						
Shirahama	10102201	0.704254 ± 0.000012	0.512783 ± 0.000010			
Monogenetic volcano						
Aojili	10102202	0.704165 ± 0.000010	0.512810 ± 0.000009			
Sumiyoshi	10102203	0.704177 ± 0.000015	0.512823 ± 0.000011	18.260 ± 0.012	15.547 ± 0.011	38.368 ± 0.026

Analytical errors are quoted at 2σ.

ratios are 61.33−68.56 wt. %, 1.15−2.72 wt. %, and 2.40−4. 12, respectively. Based on the relationships between SiO_2 contents and FeO*/MgO ratios, these lavas are classified into the calc-alkaline series defined by Miyashiro (1974). The K_2O contents in these lavas range from 1.65 to 2.55 wt. %, and fall within the medium-K classification field of Le Maitre *et al*. (1989). The basalt samples are also classified as medium-K volcanic rocks. Overall, the obtained whole-rock major element compositions are in good agreement with the relevant appeared in the previous geochemical studies on these rock suites (*e.g*., Kubotera, 1981; Yanagi *et al*., 1991; Arakawa *et al*., 1998; Uto *et al*., 2005).

The whole-rock trace element compositions determined in this study are listed in Table 2 and also plotted together with the potassium (K) and phosphorus (P) contents as MORB-normalized spider diagrams in Fig. 3. Pronounced negative Nb spikes are clearly recognized for all the samples, and Rb and K tend to be the most enriched elements relative to MORB. In addition, the Rb/Nb and K/Nb ratios are relatively high, being consistent with the values observed in island arc volcanic rocks (*e.g*., Wood *et al*., 1979; Perfit *et al*., 1980).

The whole-rock Sr-Nd-Pb isotopic compositions for the above mentioned samples are listed in Table 3 and presented in Figs 5 and 6. The Sr-Nd-Pb isotopic compositions of the Sakurajima post-caldera lavas are 18.355−18. 402 for $^{206}Pb/^{204}Pb$; 15.534−15.591 for $^{207}Pb/^{204}Pb$; 38. 485−38. 667 for $^{208}Pb/^{204}Pb$; 0. 705136−0. 705556 for $^{87}Sr/^{86}Sr$; and 0.512489−0.512561 for $^{143}Nd/^{144}Nd$ (Table 3). In contrast, the isotopic compositions determined for the pre-caldera basalt samples in this study are less radiogenic than those determined for the andesitic to dacitic post-caldera lavas (Table 3).

5. Discussion

5−1 Constraints on the origin of primary magmas of mantle origin

One of the main reasons for investigating the trace element compositions of the lavas is to elucidate the mechanisms behind the generation of the primary magmas for the Sakurajima volcano. The MORB-normalized trace element patterns for these lavas display substantial enrichments of fluid mobile elements such as Rb, K, and Pb, while showing also pronounced depletions in Nb (Fig. 3). These characteristics are generally recognized within volcanic rocks originating from arc magmas, occurring above subduction zones, and is often explained by the addition of aqueous fluid from the subducting oceanic plate to the overlying mantle wedge; the source region of arc magmas (*e.g*., Miller *et al*., 1994; Shibata and Nakamura, 1997). In the case of Sakurajima volcano, it seems likely that aqueous fluids released from the subducting PSP slab would have lowered the solidus of the overlying mantle wedge, causing partial melting to take place at depth there, and ultimately leading to the surface/near-surface magmatic activity to develop the Sakurajima volcano.

Similarly to the case with the NE Japan (*e.g.* Shibata and Nakamura, 1997; Sakuyama and Nesbitt, 1986), the geochemical characteristics for the mantle wedge beneath the Sakurajima also resemble to those for the MORB type mantle. As shown in Fig. 4, the Zr/Nb ratios for the mafic magma of the Sakurajima volcano and its adjacent area mostly come within the values for the lavas of the NE Japan. Indeed, the ratios are somewhat lower than the values for the MORB, but the obtained values are much closer to the MORBs (ave; 32) than the relevant for the OIBs (5.8; Fig. 4), although the ratio of basalt from Aojiki show the similarity to that of the OIB's.

The tendency that Zr/Nb ratio of the andesites and dacites from Sakurajima volcano decrease slightly with

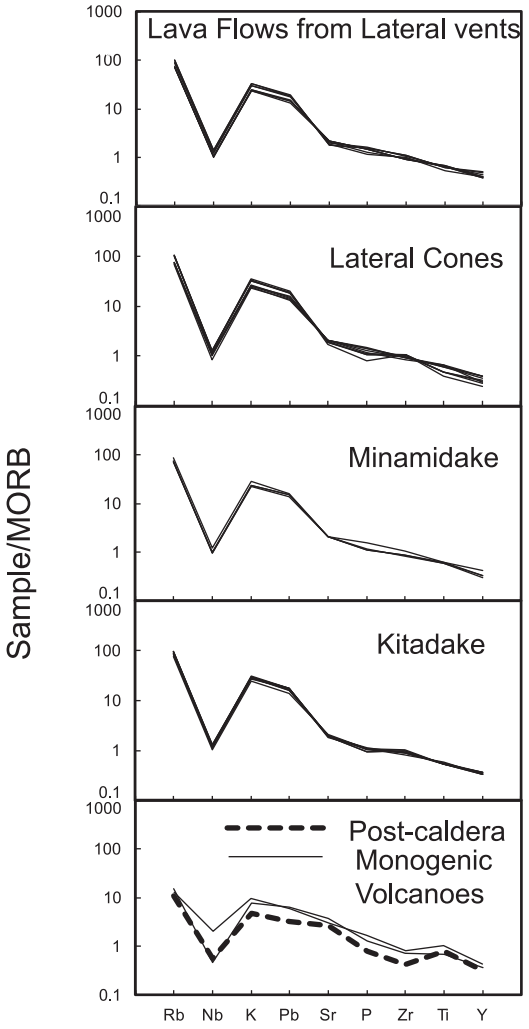

Fig. 3. MORB-normalized trace element patterns. The normalizing values are from Sun and McDonough (1989).

increasing Nb content might be due to incorporation of continental crustal materials into the magma source region, or assimilation of such crustal materials into the basaltic parental magma. As shown in Fig. 4, all the Sakurajima andesitic to dacitic volcanic rocks plot on or close to the mixing line (thick black line) between average continental crust and pre-caldera basalts in this region

The Sr-Nd-Pb isotopic compositions of all of Sakurajima lavas plot close to the two-component mixing curves between MORB-type mantle and sediments of the PSP (Fig. 5). This is well reconciled with the view based on trace element compositions that PSP slab-derived fluids were added to the mantle wedge prior to magma generation. However, from the view more in detail, the isotopic compositions for the basalt samples fall nearly on the above mentioned mixing curves, with distinctively high $^{143}Nd/^{144}Nd$ and low $^{208}Pb/^{204}Pb$ ratios relative to the post-caldera lavas (Figs 5a and 5b). This observation suggests that considerable amounts of continental crust materials mixed with basaltic parental magma. This view is compatible with our interpretation for the whole rock Zr and Nb contents and also for Sr-Nd-Pb isotopic compositions.

5−2 Sr-Nd-Pb isotope constraint for the crustal materials

The Sr-Nd-Pb isotope mixing relationships of the basement sedimentary rocks (Cretaceous Shimanto Group) with basaltic and andesitic magmas of Sakurajima volcano are examined to better understanding for the crustal materials contributed to the genesis of Sakurajima magma (Fig. 5). The sedimentary rocks of Shimanto Group are considered as one of the possible crustal source materials in the addition to the lower and upper crust (Yanagi *et al.*, 1991; Arakawa *et al*., 1989). Hosono *et al*. (2003) reported major, trace and Sr-Nd-Pb isotopic compositions of Shimanto sedimentary rocks. The isotope ratios of the Shimanto sedimentary rocks shows wide ranges of variations, so we used the data of most depleted (lowest Sr and Pb and highest Nd isotope ratios) sample (4 W4, Hosono *et al*., 2003) and enriched (highest Sr and Pb and lowest Nd isotope ratios) sample (1 WL4, Hosono *et al*., 2003) for the mixing calculations (Fig. 5).

The different two isotopic components are required as the crustal source of the Sakurajima magma from the Sr-Nd-Pb isotope mixing relationships. It is clear that andesite to dacite lavas of Sakurajima volcano are affected with crustal materials, because the Sr and Nd isotope ratios are differed from the mixing line of the subducted slab and the mantle wedge and are plotted near on the mixing line of 4 W4 and Sumiyoshiike basalt, which can represent the primary magma of Sakurajima magmas (line S in Fig. 5a). However, the trend of Sr-Nd isotope ratios of Sakurajima lava, especially two dacite lavas (10102109 and 10102112), seems to differ from the line S, and are closed to the mixing curve of Showa andesite and 1 WL4 (line S' in Fig 5a). Although most of the Pb isotope ratios of Sakurajima lavas lie on closed to the mixing line S, like as Sr-Nd isotope system, the ratios are also plotted on the slab-mantle wedge mixing line (Fig. 5b). Furthermore, the Pb isotope rations of two dacite lavas (10102109 and 10102112) show similar trend to the mixing line S' (Fig. 5b). In the Sr-Nd isotope system, it can be possible to draw mixing lines of S and S' by single isotopic component of crustal material with changing Sr/Nd abundance ratio, but it is impossible in the Pb isotope system (e.g., Shibata and Nakamura, 1997). Therefore, at least two different enriched isotopic components are required to explain the variations of Sr-Nd-Pb isotopic compositions. Although lower and upper crustal materials have to be examined as a

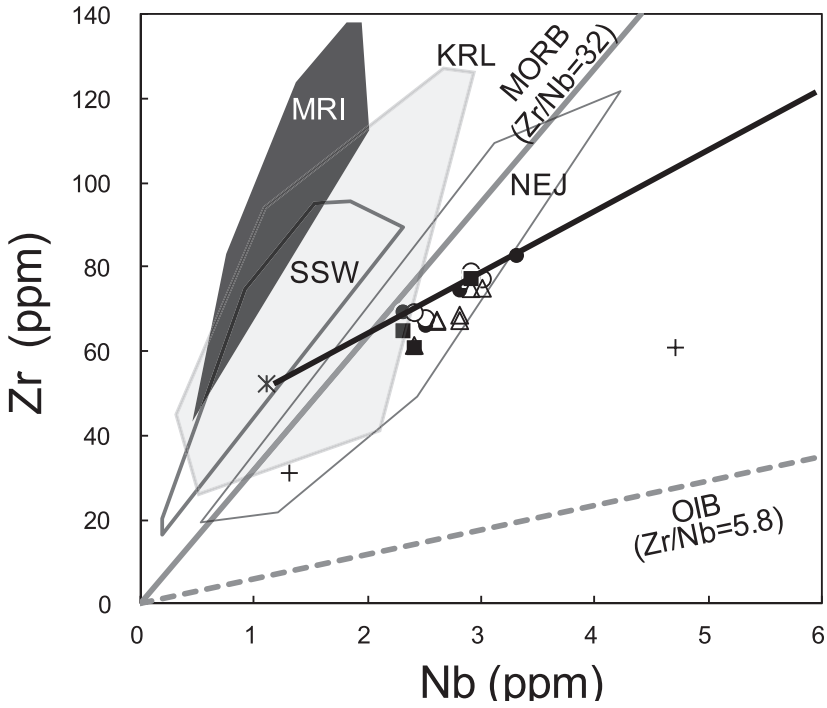

Fig. 4. Nb versus Zr concentration showing data for Sakurajima volcano (and nearby basalts). Symbols are the same as in Fig. 2. The compositional ranges of Zr and Nb from arc lavas from the Mariana (MRI), Kurile (KRL), South Sandwich (SSW), and Northeastern Japan (NEJ) arcs are shown as geochemical domains, and reference lines depicting MORB and OIB compositional trends are also shown (data are from Shibata and Nakamura (1997) and references therein). The solid black line represents a mixing line between the pre-caldera basalt composition and average continental crust (Weaver and Tamey, 1984).

crustal source, no available comprehensive data of the isotopic composition from the area closed to the Sakurajima volcano can be found. Therefore, we concluded that the Shimanto sedimentary rocks, of which Sr-Nd-Pb isotopic composition heterogeneous, can be a crustal source for Sakurajima lavas.

5−3 Genetic relationship between high- and low-P groups

The dacites of 10102109 and 10102112 show different trends of major element compositions from those of the other lavas from Sakurajima volcano, especially P_2O_5 and TiO_2. To help elucidate detailed investigation of geochemical evolution of Sakurajima magma, here after, we have subdivided our samples into high-P ($P_2O_5 > 0.15$ wt. %) and low-P ($P_2O_5 < 0.15$ wt.%) geochemical groups.

The variations of major and modal compositions can be explained by mixing between andesite magma and dacite magma. This is consistent with the previous studies (e.g., Yanagi *et al*., 1991; Arakawa *et al*., 1998). It can be suggested that the lavas of high- and low-P groups are generated by different magmatic processes judged from the variations of SiO_2, TiO_2 and P_2O_5 concentrations and $^{87}Sr/^{86}Sr$ ratios against to the modal abundance of Pl (Fig. 6). The modal abundance of Pl in lavas of Sakurajima volcano strongly correlates with major oxide contents and isotopic ratios, and the low-P and high-P groups also appear to show distinctly different trends (commonly sloping in opposite directions; Fig. 6). As shown in Fig. 6, the concentrations of TiO_2 and P_2O_5 decrease systematically with decreasing modal Pl in the low-P group, whereas the corresponding concentrations for the high-P group either increase or remain at constant values with decreasing modal Pl. Both the low-P and high-P lavas show less distinctive and comparatively broader negative correlations of SiO_2 versus modal abundance of Pl, and the SiO_2 contents of the low-P rocks are slightly higher than those of high-P rocks at >20% modal abundance of Pl. Furthermore, the Sr isotopic ratios of the low-P and high-P lavas show similar trends with respect to SiO_2 content, whereby low-P samples that have <20 modal% of Pl have distinctly high ratios ($^{87}Sr/^{86}Sr > 0.7055$), while the high-P rocks have lower ratios ($^{87}Sr/^{86}Sr < 0.7053$) (Fig. 7). These observations indicate that evolution both of high- and low-P groups had started from similar andesite magma,

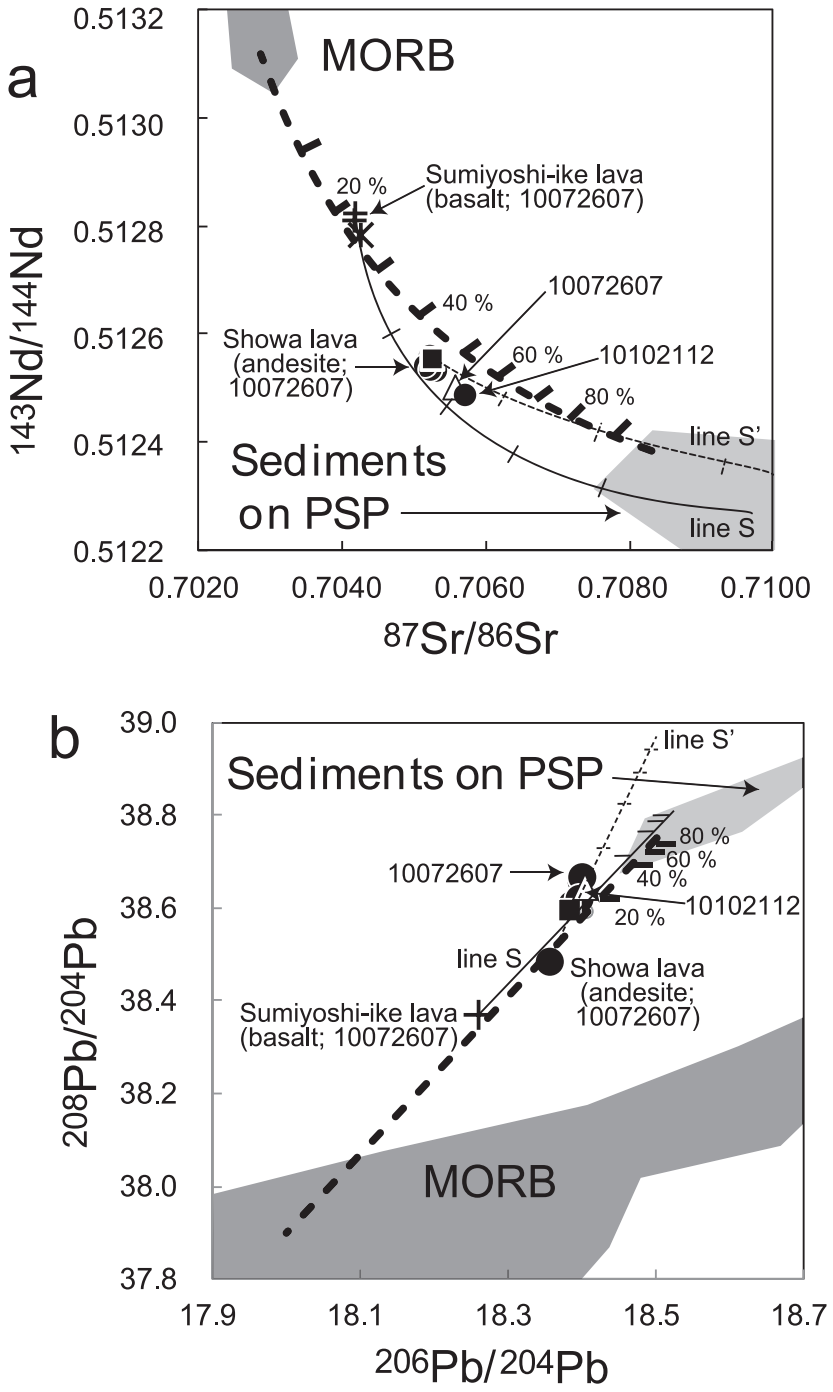

Fig. 5. Variation diagrams displaying $^{87}Sr/^{86}Sr$ versus $^{143}Nd/^{144}Nd$ (a) and $^{208}Pb/^{204}Pb$ versus $^{206}Pb/^{204}Pb$ (b). The compositional ranges of MORB and PSP sediments are also shown for reference. Symbols are the same as in Fig. 2. The dashed lines represent mixing curves between MORB and PSP sediment compositions. Tick marks along the mixing curves represent proportions of PSP sediment. Data for MORB and PSP sediments are from Shibata and Nakamura (1997) and Shimoda *et al*. (1998).

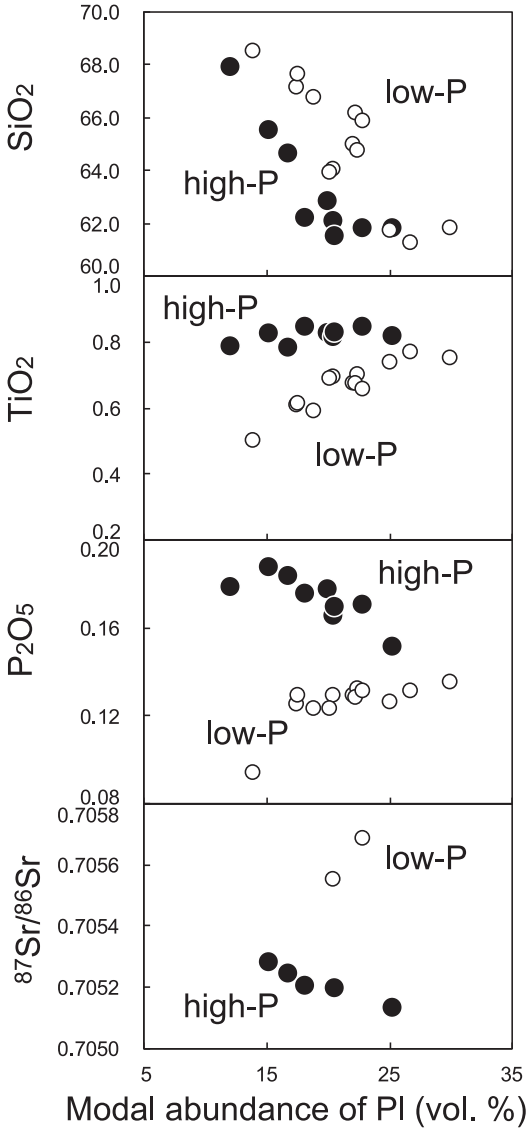

Fig. 6. Modal abundance of Pl versus SiO_2, TiO_2, and P_2O_5 concentrations, as well as $^{87}Sr/^{86}Sr$ isotopic ratios.

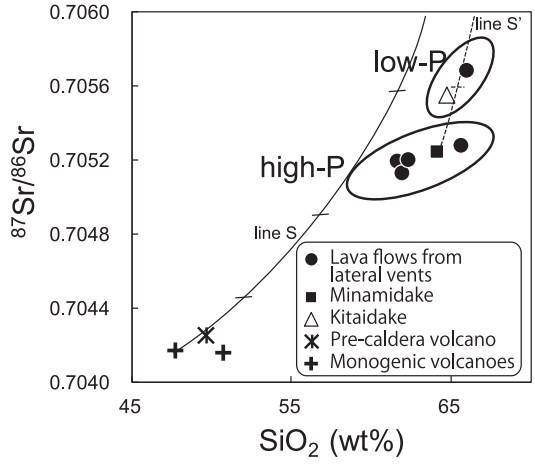

Fig. 7. SiO_2 (wt. %) versus $^{87}Sr/^{86}Sr$ isotopic ratio. Symbols are the same as in Fig. 2.

and the andesite magma mixed with the different acidic magma resulting in two different paths of magmatic processes.

The $^{87}Sr/^{86}Sr$ values of the volcanic rocks increase with increasing SiO_2 contents. However, the data are not plotted on simple mixing curve (line S in Fig. 7) between the Shimanto sedimentary rock (1 WL4, Hosono *et al*., 2003) and basalt (Fig. 7). Therefore, it is unlikely that the andesite end-member magma of Sakurajima volcano were simply produced by mixing between the basaltic magma and the crustal materials. Alternatively, the process, such as assimilation and fractional crystallization (AFC, DePaolo, 1981) from the basaltic magma is required to produce the andesite magma.

The relation of SiO_2 and $^{87}Sr/^{86}Sr$ ratio (Fig. 7) also suggests that the low-P group can be generated by the mixing between high-P andesite magma and crust derived material. The low-P group lies on the mixing line between andesite (high-P) and 4 W4 of Shimanto sedimentary rock (line S' in Fig. 7). Therefore, sedimentary rocks in the upper crust can be an end-member of the mixing. However, high-P group trend is defer from the mixing line S', but high-P group cannot be explained by this binary mixing. Arakawa *et al*. (1998) reported that the mixing line between basalt and granitic rock beneath Sakurajima volcano shows similar trend of line S. This indicates that the granitic rocks or melt generated from the granitic rock also cannot be an end-member of high-P group. Therefore, alternative process, such as assimilation and fractional crystallization (AFC, DePaolo, 1981) is again required to produce dacite end-member to produce the trend of high-P group.

5−4 Diversity and genesis of low- and high-P groups

Both the low-P and high-P lavas are observed within all of the volcanostratigraphic successions, with the exception of Kitadake, and the abundance of low-P lavas seems to decrease systematically with time (Table 1). Lavas of the high-P group are mostly distributed in the central and southern part of Sakurajima volcano, and to some extent are surrounded by low-P lavas (Fig. 1). Arakawa *et al*. (1998) proposed that dacitic magmas intruded an andesitic magma chamber, which was situated at shallower depths than the dacitic magmas, in order to enable the mixing of andesite and dacite magmas. However, the present results indicate that the dacitic magmas that occur beneath Sakurajima volcano are heterogeneous (low- and high-P),

and that the heterogeneity shows clear systematic spatio-geochemical variations (Fig. 1). If these dacitic magmas first originated from deeper levels and then interacted with a single andesitic magma, then it seems unlikely that the distinctive spatial distributions of low-P and high-P rocks (Fig. 1) would actually arise. Furthermore, dacitic magmas are more buoyant than andesitic magmas.

On the other hand, the observed heterogeneity (low- and high-P) of the dacitic magmas might have arisen due to heterogeneity within a mono-dacite magma chamber, or by the occurrence of multiple dacite magmas. The distinctive spatial distributions of low-P and high-P lavas (Fig. 1) support the existence of multiple dacitic magma chambers beneath Sakurajima volcano. Therefore, we conclude that at least two different dacitic magma chambers exist beneath Sakurajima volcano at relatively shallow levels in the crust and that andesitic magmas arose from deeper levels and then intruded into the dacitic magma chambers. A similar petrogenetic mechanism was recently proposed by Nakagawa *et al*. (2011) for the origin of the Sakurajima lavas. Ultimately, the inferred different geochemical characteristics of the low- and high-P dacitic magma chambers might have arisen by AFC processes taking place within heterogeneous crust (DePaolo, 1981).

To explain the genesis of such silicic magmas in this tectonic setting, several petrogenetic models have been proposed; 1) fractional crystallization of mafic magma with crustal assimilation (AFC model) (*e. g*., DePaolo, 1981; Caffe *et al*., 2002; Reagan *et al*., 2003), 2) partial melting of basaltic lower crust (*e. g*., Takahashi, 1986; Bead and Lofgren, 1991), and 3) partial melting of basaltic rocks that were emplaced in the lower crust a long time prior to the actual silicic magma activity (*e.g*., Sisson *et al*., 2005; Ban *et al*., 2007). Ban *et al*. (2007) invoked model 3 in order to explain arc magmatism in Northeastern Japan on the basis of relatively homogeneous Sr isotopic compositions recorded throughout the entire sequence of volcanic activity. In contrast, relatively large variations of Sr-Nd-Pb isotopic compositions are observed throughout the Sakurajima volcanostratigraphic succession, suggesting that the lower crust beneath the studied area is similar to relatively old crust having high Sr and Pb, and low Nd isotopic ratios. It has also been suggested that lower crustal materials are eventually consumed, if continual long-lived magma production occurs nearby (*e.g*., Hildreth and Wilson, 2007). If this view is correct, then old crust beneath Sakurajima volcano will become increasingly consumed, and eventually replaced by solidified basaltic magmas. This would also seem to suggest that the stage of volcanic activity taking place at Sakurajima volcano is somewhat younger than that of Northeastern Japan. Furthermore, AFC processes, in addition to crustal assimilation processes, appear to be the dominant factors controlling silicic magma production, based on the documented petrological, geochemical, and isotopic data recorded in the post-caldera lavas of Sakurajima volcano.

6. Conclusions

The depletion of Nb and enrichment of Rb, K, and Pb, which are typical geochemical features of arc magmas formed in subduction zone settings, are documented here in lavas from Sakurajima volcano. On the basis of these observed similar trace element compositions, we have deduced that the magmatism associated with this Sakurajima volcanic activity was triggered by the addition of fluids to the mantle wedge by the underlying subducting oceanic plate. We also conclude that the mantle wedge that occurs beneath the studied area is composed of MORB-type mantle, based on the similar Zr/Nb ratios in the mafic magma to that of MORB. The concentrations of Zr and Nb of andesite and dacite of the Sakurajima lavas are plotted along a mixing line of the basaltic magma and average continental crust. In addition, the Sr, Nd, and Pb isotopic compositions of the mafic magmas plot close to a mixing curve connecting MORB-type mantle and sediments of the PSP, and those of andesite to dacite lavas depart from the mixing curve along a direction of becoming more radiogenic. Collectively, these observations have led us to the following petrogenetic interpretations; 1) subducted sediments contributed to the chemical composition of the aqueous fluids derived from the PSP that infiltrated the overlying mantle wedge, 2) along with their inherited trace element compositions, the primary magmas of Sakurajima volcano were generated by the partial melting of MORB-type mantle wedge, which was metasomatized by aqueous fluids originating from the dehydrating subducting PSP slab and 3) the assimilation of crustal materials also played a role in contributing to the chemical and magmatic evolution of the studied lavas. From the Sr-Nd-Pb isotopic compositions, at least two isotopic components are required as crustal materials to explain the isotope variations of Sakurajima andesitic to dacitic magmas. Although one of the crustal component is not well constraint, but the sedimentary rocks of Shimanto Group can be the other crustal component.

The linear relationships observed on plots of SiO_2 versus most of other major element oxides suggest that magma mixing was involved in the production of the post-caldera lavas of Sakurajima volcano. Furthermore, the geochemical relationships observed on plots of SiO_2 versus TiO_2, P_2O_5, and $^{87}Sr/^{86}Sr$ suggest that the observed variations of major elements cannot be explained using only a simple binary mixing model, because two distinct trends can be observed in these diagrams. Similar conclusions were presented in previous studies (*e. g*., Yanagi, 1991; Arakawa *et al*., 1998; Uto *et al*., 2005). To explain the compositional variations, three end-members are necessary, high-P andesite and dacite, and low-P dacite, and the AFC process is required for generating andesite and dacite end-members. Another important

observation made in this study is that rock samples grouped as low-P (low P_2O_5 content) versus high-P (high P_2O_5 content) exhibit remarkably different trends on plots of plagioclase modal abundance versus SiO_2, P_2O_5, and TiO_2 concentrations and $^{87}Sr/^{86}Sr$ ratios. The Sr isotopic ratios of the low-P rocks are also high compared with those of the high-P suite of lavas. These contrasting low-P and high-P lavas also show distinctive spatial (map pattern) distributions across the Sakurajima study area. From these collective observations, we suggest that multiple dacitic magma chambers are required in the petrogenesis of these geochemically and isotopically diverse lava successions.

Acknowledgments

We thank J. Yamamoto, Y. Shitaoka, Y. Kameishi and M. Miyoshi for their valuable help and advice with regards to the experiments. We also appreciate the suggestions provided by N. Tsuchiya pertaining to petrographic studies. In addition, we are grateful to H. M. Helmy for helping to improve the manuscript. We also greatly appreciate the critical and constructive comments provided by A. Fujinawa and an anonymous reviewer. M. Ban is deeply acknowledged for his helpful and efficient handling of our manuscript. Part of this work was facilitated by a Grant-in-Aid for Scientific Research (Ministry of Education, Culture, Sports, Science and Technology, Japan) awarded to T. Shibata, as well as a Grant for Institution Collaboration (IGS, Kyoto University).

References

Arakawa, Y., Kurosawa, M., Takahashi, K., Kobayashi, Y., Tsukui, M. and Amakawa, H. (1998) Sr-Nd isotopic and chemical characteristics of the silicic magma reservoir of the Aira pyroclastic eruption, southern Kyushu, Japan. *J. Volcanol. Geotherm. Res*., **80**, 179−194.

Ban, M., Hirotani, S., Wako, A. Suga, T. Iai, Y., Kagashima, S. Shuto, K. and Kagami, H. (2007) Origin of felsic magmas in a large-caldera-related stratovolcano in the central part of NE Japan -Petrogenesis of the Takamatsu volcano. *J. Volcanol. Geotherm. Res*., **167**, 100−118.

Beard, J. S. and Lofgren, G. E. (1991) Dehydration melting and water saturated melting of basaltic and andesitic greenstones and amphibolites at 1, 3, and 6.9 kb. *J. Petrol*., **32**, 365−401.

Caffe, P. J. Trumbull, R. B., Coira, B. L. and Romer, R L. (2002) Petrogenesis of early Neogene magmatism in the Northern Puna; implications for magma genesis an crustal processes in the Central Andean Plateau. *J. Petrol*., **43**, 907−942.

DePaolo, D.J. (1981) Trace element and isotopic effects of combined wallrock assimilation and fractional crystallization. *Earth Planet. Sci. Lett*., **53**, 189−202.

Fukuyama, H. (1978) Geology of Sakurajima volcano, southern Kyushu. *J. Geol. Soc. Japan*, **84**, 309−316 (in Japanese with English abstract).

Fukuyama, H. and Ono, K. (1981) Geological map of Sakurajima volcano 1: 25,000. *Geol. Map Volcanoes, Geol. Surv. Japan*, **1**, 1−8 (in Japanese).

Furukawa, K., Miyoshi, M., Shinmura, T., Shibata, T and Arakawa, Y (2009) Geology and petrology of the pre-Aso volcanic rocks distributed in the NW wall of Aso Caldera: eruption style and magma plumbing system of the pre-caldera volcanism. *J. Geol. Soc. Japan*, **115**, 658−671 (in Japanese with English abstract).

Gregg, P. M., deSilva S. L., Grosfils, E.B. and Parmigiani, J. P. (2012) Catastrophic caldera-forming eruptions: Thermo mechanics and implications for eruption triggering and maximum caldera dimensions on Earth. *J. Volcanol. Geotherm. Res*., **241−242**, 1−12.

Hildreth, W. and Wilson, C.J.N. (2007) Compositional zoning of the Bishop Tuff. *J. Petrol*., **48**, 951−999.

Hosono, T., Nakano, T. and Murakami, H. (2003) Sr-Nd-Pb isotopic compositions of volcanic rocks around the Hishikari gold deposit, southwest Japan: implications for the contribution of a felsic lower crust. *Chemi. Geol.*, **201**, 19−36.

Inoue, H., Itaya, T. and Tatsumi, Y. (1994) Petrography, K-Ar ages and chemistry of Yoshino-dai lavas in the Aira caldera. *Bull. Disaster Prevention Res. Inst., Kyoto Univ.*, **44**, 175−190.

Kobayashi, T. (1982) Geology of Sakurajima Volcano: A Review. *Bull. Volc. Soc. Japan. Second series*, **27**, 277−292 (in Japanese with English abstract).

Kobayashi, T. and Tameike, T. (2002) History of Eruptions and Volcanic Damage from Sakurajima Volcano, Southern Kyushu, Japan, *The Quaternary Res*., **41**, 269−278.

Kubotera A. (1981) Field Excursion Guide to Sakurajima, Kirishima and Aso volcanoes. *IAVCEI Symposium on Arc Volcanism, Tokyo and Hakone.* Volcanological Society of Japan, Tokyo, 52p.

Le Maitre, R. W., Bateman. P., Dudek, A., Keller, J., Lameyre LeBas, M, J., Sanine, P. A., Schmid, R., Sorensen, H., Strckeisen, A., Woolly, A. R. and Zanettin, B. (1989) **A classification of igneous rocks and glossary of terms**. Blackwell, Oxford.

Lipman, P. W. (1984) The roots of ash flow calderas in western North America: windows into the tops of granitic batholiths. *J. Geophys. Res*., **89 (B10)**, 8801−8841.

Miller, M. M., Goldstein, S. L. and Langmuir, C. H. (1994) Cerium/Lead and lead isotope ratios in arc magmas and the enrichment of lead in the continents. *Nature*,**368,** 514−519.

Miyashiro, A. (1974) Volcanic rock series in island arcs and active continental margins. *Am. J. Sci*., **274**, 321−355.

Miyoshi, M., Shibata, T., Yoshikawa, M., Sano, T. Shinmura, T. and Hasenaka, T. (2011) Genetic relationship between post-caldera and caldera-forming magmas from Aso volcano, SW Japan: Constraints from Sr isotope and trace element compositions. *J. Mineral. Petrol. Sci*., **106**, 114−119.

Nakagawa, M., Matsumoto, A., Amma-Miyasaka, M. and Iguchi, M. (2011) Change of mode of eruptive activity and the magma plumbing system of Sakurajima Volcano since 20th century. *Japan Geoscience Union Meeting 2001*,

SVC050−22, Makuhari, Chiba, Japan.

Okuno, M. (2002) chronology of tephra layers in southern Kyushu, SW Japan, for the last 30, 000 years. *The Quaternary Res*., **41**, 225−236.

Pearce, J. A. (1983) Role of the sub-continental lithosphere in magma genesis at active continental margins. In *Continental Balsats and Mantle Xenoliths* (Hawkesworth, C.J. and Norry, M. J. ed.), 230−249, Natwich, UK: Shiva.

Perfit, M. R., Gust, D. A., Bence, A. E., Arculus, R. J. and Taylor S. R. (1980) Chemical characteristics of island-arc basalts: Implications for mantle sources. *Chem. Geol*., **30**, 227−256.

Reagan, M.K., Sims, K.W.W., Erich, J., Thomas, R.B., Cheng, H., Edwards, R.L., Layne, G.D., and Ball, L. (2003) Time-scales of differentiation from mafic parents to rhyolite in North American continental arcs. *J. Petrol.*, **44**, 1703−1726.

Sakuyama, M. and Nesbitt, R. W. (1986) Geochemistry of the Quaternary volcanic rocks of the Northeastern Japan arc. *J. Volcanol. Geotherm. Res*., **29**, 413−450.

Smith, R. L. and Bailey, R. A. (1968) Resurgent cauldrons. *Geological Society of America Memoirs*, **116**, 613−662.

Shibata, T. and Yoshikawa, M. (2004) Precise isotope determination of trace amounts of Nd in ultramafic rock samples. *J. Mass Spec. Soc. Japan*, **52**, 317−324.

Shibata, T. and Nakamura, E. (1997) Across-arc variations of isotope and trace element compositions from Quaternary basaltic volcanic rocks in northeastern Japan: implications for interaction between subducted oceanic slab and mantle wedge. *J. Geophys. Res*., **102**, 8051−8064.

Shibata, T., Yoshikawa, M. and Sugimoto, T. (2007) Semi-automatic Chemical Separation System for Sr and Nd isotope analyses. *J. Mineral. Petrol. Sci*., **102**, 208−301.

Shimoda, G., Tatsumi, Y., Nohda, S., Ishizaka,, K. and Jahn, B. M. (1998) Setouchi high-Mg andesites revisited: geochemical evidence for melting of subducting sediments. *Earth Planet. Sci. Lett*., **160**, 479−492.

Sudo, M., Uto, K., Miki, D. and Ishihara, K. (2001) K-Ar dating of volcanic rocks along the Aira caldera rim: Part 2 - Volcanic history of western and northwestern area of caldera and Sakurajima volcano. *Ann. Disas. Prev. Res. Inst., Kyoto Univ*., **44**, 205−316.

Sun, S. S. and McDonough, W. F. (1989) Chemical and isotopic systematics of oceanic basalts: implications for mantle composition and processes. In *Magmatism in the Ocean Basins* (Saunders, A. D. and Norry, M. J. ed.), 313−345, Geol. Soc., Spec. Pub. **42**, London.

Sisson, T. W., Ratajeski, K., Hankins, W. B. and Glazner, A. F. (2005) Voluminous granitic magmas from common basaltic sources. *Contrib. Mineral. Petrol*., **148**, 542−565.

Takahashi, E. (1986) Genesis of calc-alkali andesite magma in a hydrous mantle-crust boundary: Petrology of lherzolite xenoliths from the Ichinomegata crater, Oga peninsula, northeast Japan, part II. *J. Volcanol. Geotherm. Res*., **29**, 355−395.

Uto, K., Miki, D., Nguen, H., Sudo, M., Fukushima, D. and Ishihara, K. (2005) Temporal Evolution of Magma Composition in Sakurajima Volcano, Southwest Japan. *Ann. Disas. Prev. Res. Inst., Kyoto Univ*., **48 B**, 341−348 (in Japanese with English abstract).

Weaver, B. L. and Tamey, J. (1984) Major and trace element composition of the continental lithosphere. In *Physics and Chemistry of the Earth* (Pollack, H. N. and Murthy, V. R. eds.), 39−68, Pergamon, Oxford,.

Wood, D. A., Joron, J. -L., Treuil, M., Norry, M. and Tarney, J. (1979) Elemental and Sr isotope variations in basic lavas from Iceland and the surrounding ocean floor. *Contrib. Mineral. Petrol*., **70**, 319−339.

Yanagi, T., Ichimaru, Y. and Hirahara, S. (1991) Petro-chemical evidence for coupled magma chambers beneath the Sakurajima volcano, Kyushu, Japan. *Geochem. J.*, **25**, 17−30.

Yoshikawa, M. and Shibata, T. (2002) Sr and Nd isotopic ratios and Rb, Sr, Sm, and Nd concentrations of JB-2 rock reference material with isotope dilution method. *Ann. rep. Inst. Geoth. Sci.*, 30−31, 2002.

(Editorial handling Masao Ban)

桜島火山第四紀溶岩の地球化学及び Sr-Nd-Pb 同位体組成を用いたマグマ起源の解明

柴田知之・鈴木　淳・芳川雅子・小林哲夫・味喜大介・竹村恵二

始良カルデラの後カルデラ期の桜島火山に産する溶岩，及び，桜島周辺に産する前カルデラ期と単成火山の玄武岩について，主要元素・微量元素，ストロンチウム (Sr)・ネオジム (Nd)・鉛 (Pb) 同位体組成を測定した．桜島火山の溶岩は斜方輝石，単斜輝石，斜長石（稀にかんらん石）の斑晶を持つ，安山岩及びデイサイトである．微量元素組成から，島弧マグマの典型である Nb の枯渇，Rb・K・Pb の富化が観察され，マントルウェッジに水に富む流体が付加されたことを示す．Zr/Nb 比は MORB の比に類似し，また，Sr・Nd・Pb 同位体組成は MORB 型マントルとフィリピン海プレート上の堆積物の混合曲線付近にプロットされる．これらは，桜島及びその周辺のマグマは，MORB 型のマントルが沈み込んだフィリピン海プレート起源の流体の付加を受け部分溶融して生成したことを示す．さらに，Zr/Nb 比や同位体組成が，前者は MORB の値から，後者は MORB とフィリピン海プレート上の堆積物との混合曲線から，それぞれ地殻物質の値へ向かう傾向を示すことから，地殻物質がマグマの化学組成に影響を与えた可能性が指摘される．Sr-Nd-Pb 同位体組成から，少なくとも二つの地殻物質が桜島のマグマの起源に関与しており，そのうち一つは四万十層群の堆積岩を起源とすると考えられる．主要元素組成はハーカー図において，P_2O_5 と TiO_2 を除き，直線的な傾向を示す．この事から，P_2O_5 濃度をもとに，試料を low-P と high-P に区分した．Low-P と high-P は斜長石の斑晶モード組成に対する SiO_2，P_2O_5，TiO_2 濃度，及び，$^{87}Sr/^{86}Sr$ 比との間で，それぞれ異なるマグマ混合の関係を示す．また．主要元素と同位体組成の関係から，マグマ混合の両端成分を生成するには，地殻同化と結晶分化作用が同時に進行する過程(AFC)などの過程が必要であることが示された．